DOI original paper: 10.1007/978-3-031-07322-9_82

Practical experiences to know making Acoustic Emission-based SHM successful

Jonathan Liebeton and Dirk Söffker

Chair of Dynamics and Control, University of Duisburg Essen, Germany
jonathan.liebeton@uni-due.de
soeffker@uni-due.de

Abstract. The use of ultrasonic waves in the context of SHM offers methods to analyze materials and systems. Both Acoustic Emission-based approaches (passive, active) are limited by the propagation characteristics of ultrasonic waves, especially in inhomogeneous materials like carbon fiber reinforced polymers (CFRP). The use of the piezoelectric and inverse piezoelectric effect is a very accurate method of sensing and exciting ultrasonic waves. However, the transducers resonance characteristics affect the waveforms. For illustration in this contribution different excitation signals are experimentally compared in frequency domain by fast Fourier transform (FFT) and in time-frequency domain by continuous wavelet transform (CWT). Then transducers effects along the propagation path of the wave are investigated. Frequency and fiber direction dependent damping factors of ultrasonic waves in CFRP as well as the influence of the transducers are determined. The distance between sensors in a sensor network is limited by attenuation, so fiber direction must be considered. Finally, by analyzing the frequency response of the transducer, a filtering method is developed to compensate for the resonance characteristics of the transducers. Finally, a more accurate estimate of the energy released and therefore a more accurate estimate of the severity of damages/failures is proposed.

Keywords: Acoustic Emission · piezoelectric transducers · wave propagation.

1 Introduction

In recent years, efficiency has experienced a rapidly increasing interest. To increase the efficiency of a system, the weight of moving parts are decreased. Because of their strength to weight ratio fiber reinforced materials are chosen to replace heavier metal components. Fiber reinforced materials are used in transportation and construction industry. carbon fiber reinforced polymers (CFRP) is a common used material for bodywork for example in cars, trains and planes. The use in safety critical parts like fuel cells for hydrogen, liquid oxygen or methane, beams or frames is still restricted due to the material's damage behavior. Under extensive load micro-mechanical damages occur. These damages can be classified as matrix crack, delamination, debonding and fiber breakage.

In comparison to metal, a visual detection of damages is not possible in CFRP, because the fibers are embedded inside the material [1]. The detection of micro-mechanical damages inside the material is crucial, because of the non ductile behavior of CFRP the damages build up until the sudden total failure of the material. Acoustic Emission-based approaches are commonly used methods for monitoring these. These methods are divided into active and passive methods.

In active methods, ultrasonic waves are generated and send into the investigated material. The waves propagate alongside the material's boundaries, therefore the ultrasonic waves are also referred to as guided waves. The ultrasonic waves are reflected at changes in the material properties, e.g. change in stiffness or cross section. Material changes are detected by measuring and analyzing the reflected waves.

In passive Acoustic Emission-based methods the Kaiser effect is used. By exceeding material-specific stress thresholds Acousitc Emission are generated. In CFRP each damage mechanism corresponds to a specific frequency range. Fiber breakage emits compared with other damage mechanisms the highest frequencies in a range of 300 to 500 kHz [2, 3]. Characteristic frequencies of delamination are the lowest ones of all damage mechanisms in a range of 50 to 120 kHz [4, 5]. The frequencies of matrix crack and debonding, are occurring in a range between delamination and fiber breakage [3, 5].

Ultrasonic waves propagate in solids in form of longitudinal and transverse waves. While longitudinal waves oscillate in propagation direction, transverse waves oscillate perpendicular to the direction of propagation. In thin structures, Lamb waves are generated by reflections of longitudinal and transverse waves from free surfaces. Lamb waves are divided into two modes. Both modes can occur simultaneously and propagate with independent velocities. The flexural mode describes the condition in which the surfaces oscillate asymmetrically about the center plane of the structure. Symmetrical oscillations about the structure's center plane are called extensional mode. Lamb waves show dispersive behavior. Phase velocity, the velocity of a monochromatic wave, depends on the mode and frequency as does group velocity, the velocity of a group of waves with different frequencies. The amplitude of Lamb waves decreases with increasing propagation distance. The decrease is due to geometrical spreading and inner friction of the wave. These effects are mathematically described by

$$V_i = \frac{1}{\sqrt{x_i}} \cdot V_0 \cdot e^{-\alpha x_i}, \tag{1}$$

where V_i denotes the amplitude at the distance x_i to the source, V_0 the amplitude at the source, and α the attenuation coefficient [6]. Inner friction leads to an exponentially amplitude decrease dependent on the attenuation coefficient and the distance to the source.

The phase velocity depends on material stiffness, therefore also the group velocity is affected by material changes [7]. Waves which are reflected multiple times at the material's boundaries show changes in the frequency spectrum due to varying propagation distances [8]. The signals energy distribution shifts to

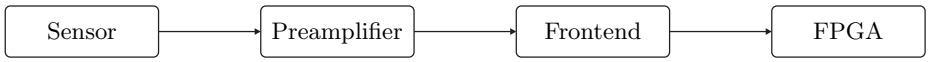

Fig. 1. Measurement chain

lower frequency ranges for increasing propagation distances [8]. Time of flight and time of arrival methods use estimates of the propagation velocity basted on the the waves frequency to calculate the source of the signal. Therefore a frequency shift leads to an inaccurate source localization. Additionally reflections produce signal interference and therefore change the original waveform.

The investigation objective is to show aspects of Lamb waves propagation behavior in CFRP. Additionally the transfer behavior of piezoelectric transducers is examined. The transducers frequency dependent signal amplification is compensated using a filter based on inverse frequency response. Signal attenuation due to additional sensors in the propagation path is calculated.

2 Experiments

Two experiments are conducted to investigate the behavior of piezoelectric transducers and propagation of Lamb waves. The measurement chain shown in figure 1 is used the measure Lamb waves and transform these into digital signal for subsequent signal analysis. While used as sensors piezoelectric transducers convert mechanical stress of the attached surface into electrical voltage. By using the inverse piezoelectric effect the transducers convert an electrical voltage to mechanical stress.

Oscillations of the piezoelectric material excite Lamb waves in the adjacent material. This requires a stiff bonding of transducer on the attached surface. The analog measurement is preamplified to increase the signal to noise ratio. A frontend is used to embed a field programmable gate array (FPGA) card. The FPGA card is the central element of the measurement chain. Analog input signals are A/D converted with a sample rate of 4 MHz.

In both experiments piezoelectric transducers are used as actuators to excite Lamb waves. An arbitrary signal generator is used to generate a signal sequence. In each sequence a frequency range of 10 to 550 kHz is covered. Starting with 10 kHz the frequency is increased in steps of 10 kHz. A Hann window is applied to a sine signal with six cycles to increase the accuracy of the frequency spectrum. Using an internal trigger, the signal is generated every 100 ms with a peak-to-peak amplitude of 5 V.

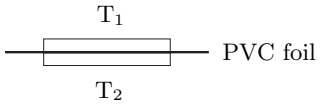

Fig. 2. Sensor behavior experiment

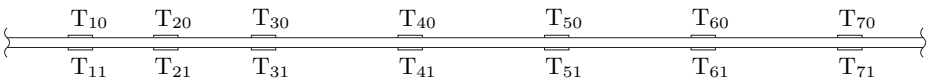

Fig. 3. Attenuation experiment

In the first experiment two transducers are bonded directly together. A thin polyvinyl chloride (PVC) foil is used as electrical isolation between both transducers, as shown in figure 2. While transducer T_2 is used as an sensor, transducer T_1 is connected to the signal generator which sends the signal sequence.

In the second experiment, transducers are attached in co-located pairs on the top and bottom side of a CFRP plate. The transducers T_{10} and T_{11} are used as actuators to send the signal sequences. The fiber layers of the CFRP plate are oriented in 0° and 90°. The sensors T_{20}, T_{21} to T_{70}, T_{71} are bonded to the CFRP plate in descending order. Starting with the transducer pair T_{70} and T_{71}, a free propagation path between actuators ans sensors is guaranteed. After completing the signal sequence, a new sensor pair is attached to the surface. The distance between each sensor pair and the actuators is listed in table 1. The signal sequence is also measured for configurations with unused transducers in the propagation path between measuring sensors and Lamb wave exciting actuators.

3 Methods

The measured data are analyzed by applying different signal processing and filtering methods. The used methods are briefly introduced in the following sections. A band-pass filter is applied to all measurements to eliminate mains hum. In order to analyze the signal's frequency spectrum fast Fourier transform (FFT) is used. The Fourier transformed X_k of a discrete time signal x_n is described by

$$X_k = \sum_{n=0}^{N-1} x_n \cdot e^{-i2\pi k \frac{n}{N}}, \tag{2}$$

Table 1. Transducer positions

Sensors		Distance
T_{20}	T_{21}	35 mm
T_{30}	T_{31}	75 mm
T_{40}	T_{41}	135 mm
T_{50}	T_{51}	195 mm
T_{60}	T_{61}	255 mm
T_{70}	T_{71}	315 mm

with $k = 0, ..., N-1$. A time frequency analysis is done by calculating wavelet coefficients using continuous wavelet transform (CWT). The CWT is defined as

$$X_w(a,b) = \frac{1}{\sqrt{a}} \int_{-\infty}^{\infty} x(t) \Psi^* \left(\frac{t-b}{a} \right) dt, \tag{3}$$

with a wavelet Ψ scaled in frequency and shifted in time by the parameters a and b respectively. The re-transformation of wavelet coefficient from time frequency domain to time domain is done by applying inverse continuous wavelet transform (ICWT). The re-transformed time signal $x(t)$ is described by

$$x(t) = \frac{1}{2\pi \Psi^*} \int_{-\infty}^{\infty} \int_{-\infty}^{\infty} \frac{1}{a^2} X_w(a,b) \exp\left(i \frac{t-b}{a} \right) db \; da, \tag{4}$$

where $X_w(a,b)$ are the wavelet coefficients. The time synchronous average (TSA) $m(t)$ is calculated according to

$$m(t) = \frac{1}{N} \sum_{i=0}^{N-1} x(t + iT) \tag{5}$$

for a repeating signal $x(t)$. Noise is reduced by factor $\frac{1}{\sqrt{N}}$ with N as number of signal repetitions. The attenuation coefficient α is calculated by

$$\alpha = \left(\frac{1}{x_1 - x_0} \right) \log \left(\frac{V_0 \sqrt{x_0}}{V_1 \sqrt{x_1}} \right) \tag{6}$$

for a signal's peak amplitudes V_0 and V_1 at distances x_0 and x_1 respectively [6].

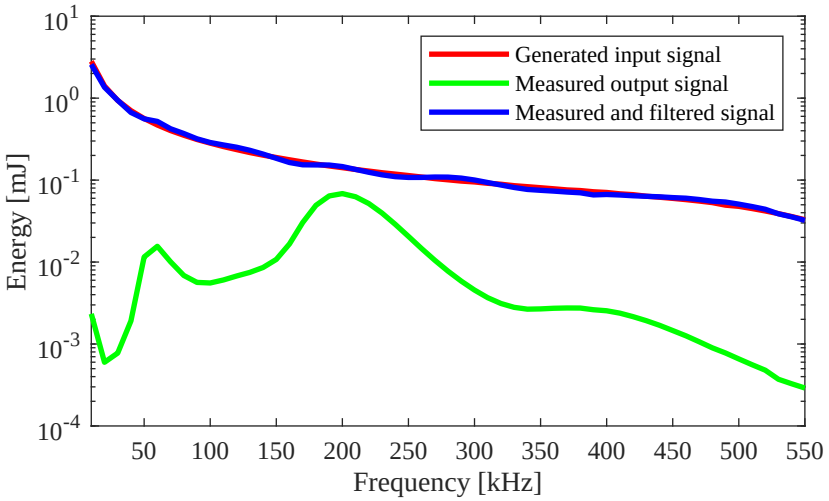

Fig. 4. Comparison of the energy of different signals (bandwidth 0 - 550 kHz)

4 Results and discussion

The frequency dependent amplification behavior of piezoelectric transducers have a significant influence on measurements. The transfer behavior is non linear with a resonance characteristic at 200 kHz in case of free oscillation. If bonded to a surface, the resonance frequency is increased (plus 0 to 25 %). For Acoustic Emissions generated by micro-mechanical damage the released energy indicates the damage severity. Because of the transducers transfer behavior an accurate estimate of damage severity is not possible. Therefore the inverse frequency

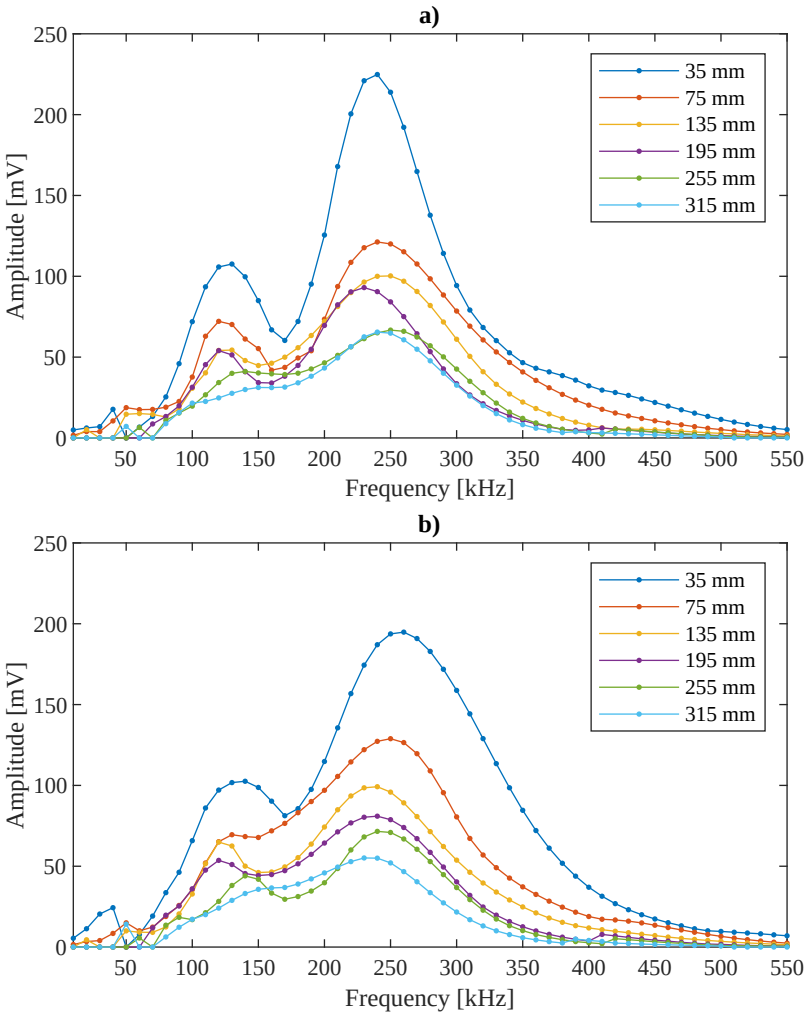

Fig. 5. Comparison of peak amplitudes on the a) top and b) bottom side of a CFRP plate

response of the transducer is used to compensate frequency dependent amplification. Measurements from the first experiment are used to establish a filter, which is applied to the signals CWT coefficients. The energy of each signal is calculated after the ICWT of the filtered coefficients.

In figure 4 the energy of signals with different frequencies are shown. A band pass filter with a frequency range of 5 and 600 kHz additionally reduces the energy of signals with a frequency of 500 kHz and higher. The energy of measured signals is showing a resonance peak at 200 kHz. A significant difference between the energy of the generated signals and the measured signals can be observed. After the filter is applied to the measured signals, a good estimation of the released energy is possible. The transducers frequency dependent transfer behavior is compensated.

In figure 5a) and 5b) the peak amplitudes on the top and bottom side of a CFRP plate of different frequencies and at different propagation distances are shown. The resonance peak can be detected at 240 and 250 kHz for top and bottom side of the CFRP at the shortest distance between sensor and actuator pair. The frequency shift towards lower frequencies is clearly visible for resonance peak in figure 5b). There are differences between figure 5a) and 5b) because of

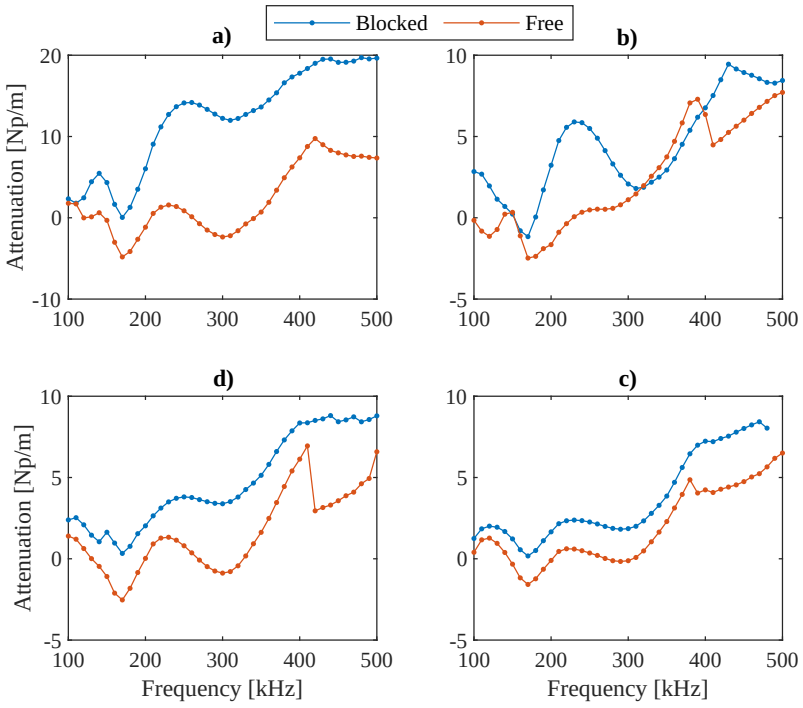

Fig. 6. Frequency dependent attenuation at a) 75 mm, b) 135 mm, c) 195 mm and d) 255 mm distance for one and none transducer pair in the propagation path

different amount of adhesive around the sensors and small position deviations of the sensor pairs.

In figure 6 the additional signal attenuation for the case, when an additional transducer pair is blocking the propagation path is shown. In case of the transducer T_{30} in figure 6a) the additional transducer in the propagation path results in a strong attenuation. Differences between the adhesive around the transducers lead to differences as shown in the figures.

5 Summary and conclusions

This contribution points out the propagation behavior of Lamb waves in CFRP, which must be considered for Acoustic Emission-based methods. The propagation behavior is strongly related to the waves frequency. The frequency decreases with increasing propagation distance, the propagation behavior is also changing. A filter approach is proposed which compensates the transfer behavior of piezoelectric transducers and offers a better estimation of the signal energy. This allows a more accurate assessment of the severity of damages. The attenuation of Lamb waves show a frequency dependent behavior. Additional transducers in the propagation path increase the attenuation significantly. Future investigations will focus on the role of reflections, i.e. the possibilities under which conditions the frequencies are shifted between input and output and which parameters are affecting this.

References

1. Rauter, F., Lammering, R.: Impact Damage Detection in Composite Structures Considering Nonlinear Lamb Wave Propagation. Mechanics of Advanced Materials and Structures, pp. 44–51 (2015)
2. Oskouei, A. R., Heidary, H.: Unsupervised acoustic emission data clustering for the analysis of damage mechanisms in glass/polyester composites. Materials & Design, pp. 416–422 (2012)
3. Hamdi, S. E., Le Duff, A.: Acoustic emission pattern recognition approach based on Hilbert–Huang transform for structural health monitoring in polymer-composite materials. Applied Acoustics, pp. 746–757 (2013)
4. Gutkin, R., Green, C. J.: On acoustic emission for failure investigation in CFRP: Pattern recognition and peak frequency analyses. Mechanical Systems and Signal Processing, pp. 1393–1407 (2011)
5. Baccar, D., Söffker, D.: Identification and classification of failure modes in laminated composites by using a multivariate statistical analysis of wavelet coefficients. Mechanical Systems and Signal Processing, pp. 77–87 (2017)
6. Asamene, K., Hudson, L.: Influence of attenuation on acoustic emission signals in carbon fiber reinforced polymer panels. Ultrasonics, pp. 86–93 (2015)
7. Petculescu, G., Krishnaswamy, S.: Group delay measurements using modally selective Lamb wave transducers for detection and sizing of delaminations in composites. Smart Materials and Structures (2007)
8. Crawford, A., Droubi, M.G.: Analysis of Acoustic Emission Propagation in Metal-to-Metal Adhesively Bonded Joints. Journal of Nondestructive Evaluation 37(2), 1–19 (2018)